

## **Electronic Supporting Information**

### **Self-Assembled Materials from Cellulose Nanocrystals Conjugated with a Thermotropic Liquid Crystalline Moiety**

Francis K. Masese<sup>†</sup>, Dennis Ndaya<sup>†§</sup>, Chung-Hao Liu<sup>§</sup>, Nicholas Eddy<sup>†§</sup>, M. Daniela Morales-  
Acosta<sup>§</sup>, Mu-Ping Nieh<sup>§</sup><sup>✉</sup>, Rajeswari M. Kasi<sup>†§</sup>

<sup>†</sup>Department of Chemistry, University of Connecticut, Storrs, CT 06269 (USA)

<sup>§</sup>Polymer Program, Institute of Material Science, University of Connecticut, Storrs, CT 06269

\* Authors to whom correspondence should be addressed.

Prof. R M Kasi: [rajeswari.kasi@uconn.edu](mailto:rajeswari.kasi@uconn.edu); Tel: +1 (860)-486-4713

## **1.1. Instrumentation**

### **1.1.1. Thermal Gravimetric Analysis (TGA)**

Thermogravimetric analysis is performed using 5-10 mg of the sample on a TGA Q500 1732 to analyze thermal properties at 20° C/min under Nitrogen.

TGA of the CNCs before and after TEMPO-mediated oxidation shows a slight reduction in thermal stability, with an onset of degradation at 275 °C and 210 °C, respectively. TGA of CNC-COO-CB12 shows two transparent regimes that align well with the degradation of the CNC and CB12-OH. The weight percent of the grafted polymer was calculated by comparing mass loss from 220 °C to 360 °C, which predominantly corresponds to CNC degradation. The mass loss from 360 to 450 °C predominantly corresponds to decarboxylation of the sample. No residual ionic liquid and DMSO are observed in these TGA measurements, indicating the lack of trapped solvents in the system.

### **1.1.2. Differential Scanning Calorimetry (DSC)**

Differential scanning calorimetry (DSC) is conducted on the TA-2920 instrument (Q-200 series) calibrated with an Indium standard. The amount of sample used is 5-10 mg, and the scanning rate is 10 °C/min. Universal Analysis software determines phase transition temperatures by the first cooling cycle and the second heating cycle.

### **1.1.3. Fourier Transform-Infrared (FT-IR)**

Infrared spectra are acquired on a Nicolet Magna-IR 560 spectrometer with a resolution of 2 cm<sup>-1</sup> and 32 scans in micro-ATR mode. The spectrometer is equipped with a Specac Quest single reflection ATR accessory containing a diamond crystal sample plate.

### **1.1.4. Wide Angle X-ray Analysis (WAXS)**

WAXS scans are performed on an Oxford Diffraction XCalibur PX Ultra (transmission mode) diffractometer with an Onyx detector (Cu-K $\alpha$  radiation 1.542 Å, double mirror focusing, 45 kV and 45 mA). The crystallinity index is calculated using the ratio of the area under the crystalline region and the total area obtained from peak fitting. Crystallite size is determined by the Scherrer equation, and the peak centered at  $\sim 23^\circ$  ( $2\theta$ ).

### **1.1.5. Small Angle X-ray Analysis (SAXS)**

SAXS experiments are performed using a two pinhole (500 and 350 $\mu$ m) Bruker NanoStar instrument with Cu-K $\alpha$  radiation (1.542 Å) produced by a turbo rotating anode. The scattered intensity is recorded on a Vantec-2000 area (2D) detector. The area detector has a resolution of 1024  $\times$  1024 pixels, located at  $\sim 28$  cm from the sample center, permitting access to scattering vectors ranging from 0.045 to 1.1 Å<sup>-1</sup>. Silver behenate (d-spacing=58.38 Å) calibrated the SAXS diffraction patterns. The 1D SAXS data is corrected for the sample transmission.

### **1.1.6. Scanning Electron Microscope (SEM)**

Images of all samples are recorded using an FEI Teneo LVSEM equipped with an ETD detector with an accelerating voltage of 5 kV at the UCONN/FEI Center for Advanced Microscopy and Materials Analysis (CAMMA). Before imaging, the film samples are prepared using solvent evaporation and sputter coating with a thin gold conductive layer. The SEM images show the top-down photos of the CNC, CNC-COOH, and CNC-COO-CB12 films

### **1.1.7. Polarized Optical Microscopy (POM)**

Olympus BX51P microscope equipped with Instec HCS410 hot stage is used to determine the optical texture of the films. The samples are placed on microscope glass slides and annealed at a temperature slightly above TLC1 and slightly below TLC2 transition temperatures for 24 h. The characteristic texture of mesophase and the aspect ratio of the CNCs are determined.

### **1.1.8. UV-Visible Spectroscopy**

UV spectroscopic data is obtained from Shimadzu UV-Vis Spectrometer (UV-2450) in reflectance mode with a 200 -900 nm wavelength range. The free-standing films (~ 0.3 mm in thickness) are prepared by solution casting on the polyimide Kapton films for 72 hours.

### **1.1.9. Solid-state cross-polarization <sup>13</sup>C NMR:**

<sup>13</sup>C NMR spectroscopy is conducted on the Bruker Avance III 400 MHz Wide Bore (WB) NMR spectrometer with a three-channel state-of-the-art system dedicated to solid samples with Magic Angle Spinning (MAS) and Pulse Field Gradient capabilities. The spectrometer is equipped with a triple resonance HXY 4 mm MAS probe and a triple resonance HFX 2.5 mm MAS probe for solids with VT from – 50 to +150 degrees Celsius running experiments with Nitrogen gas. It is also equipped with a double resonance H(F)X 5 mm Doty Scientific Pulse Field Gradient (PFG) probe with a Z-axis Great 1/40 gradient amplifier for liquid and solid samples diffusion studies.

### **1.1.10 Transmission Electron Microscopy (TEM):**

The TEM images are acquired using FEI Tecnai T12 with an accelerating voltage 80 kV. CNC, CNC-COOH, and CNC-COO-CB12 are dispersed in water with a concentration of 0.5 mg/mL. Then, 3 μL of the samples are deposited on the 200 mesh copper grids covered with carbon film. The samples are negatively stained by 0.5 wt.% of uranyl acetate before imaging. Excess fluid is then blotted with Whatman filter paper, and the grids are dried at room temperature overnight.

### 1.1.11. <sup>1</sup>H NMR:

<sup>1</sup>H NMR spectroscopy is conducted on the Bruker DMX 500 MHz NMR spectrometer with CDCl<sub>3</sub> and DMSO-d<sub>6</sub> as the lock solvents at room temperature. <sup>1</sup>H NMR chemical shifts are delineated in ppm downfield from TMS. <sup>1</sup>H NMR (500 MHz, DMSO) δ 9.35 (s, 1H), 7.93 – 7.79 (m, 2H), 7.71 (d, J = 8.5 Hz, 1H), 7.05 (d, J = 8.3 Hz, 1H), 4.18 (t, J = 7.2 Hz, 1H), 4.11 – 3.78 (m, 3H), 3.50 – 3.21 (m, 1H), 2.56 (s, 0H), 2.52 (s, 1H), 2.00 (s, 1H), 1.74 (dq, J = 21.5, 7.6, 6.9 Hz, 2H), 1.67 – 1.48 (m, 2H), 1.41 (q, J = 7.4 Hz, 1H), 1.27 (d, J = 14.7 Hz, 9H).

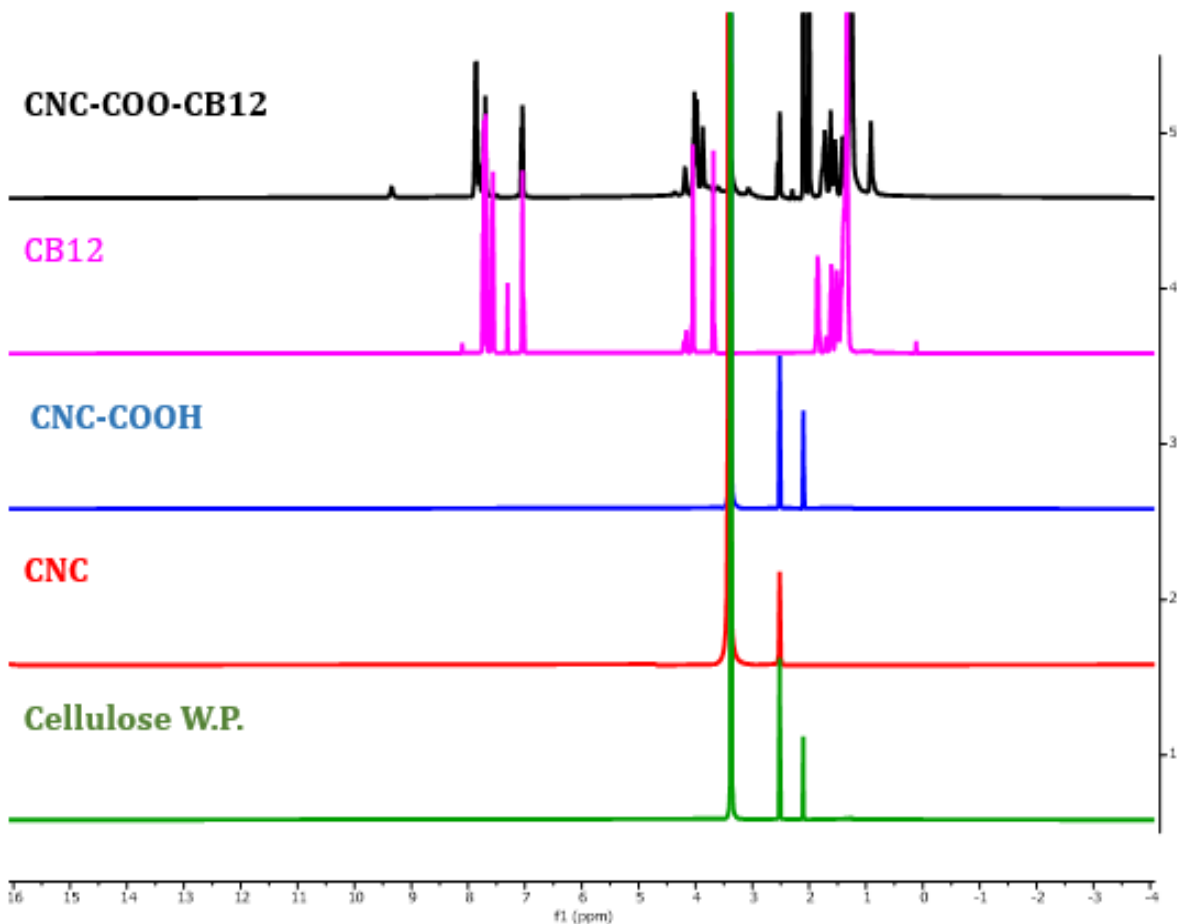


**Figure S1.**  $^1\text{H}$  NMR spectra overlay of Cellulose W.P., CNC, CNC-COOH, CB12, and CNC-COO-CB12 in  $\text{DMSO-}d_6$  at  $25^\circ\text{C}$ . The Cellulose W.P., CNC, CNCOOH, were insoluble in  $\text{DMSO-}d_6$  at  $25^\circ\text{C}$  and hence no peaks are resultant peaks appear. The appended CNCOOCB12 was soluble in  $\text{DMSO-}d_6$  at  $25^\circ\text{C}$ . The ester proton peak appears at 4.08 ppm, thus indicating the proof of functionalization. The additional peak at 9.75 ppm, indicate the presence of the proton from the carbonyl carbon (CNC-COOH). This is a proof that the degree of functionalization is less than 100 percent. Functionalization of the oxidized cellulose nanocrystals (CNC-COOH) with the CB12 improved its solubility in  $\text{DMSO-}d_6$ .

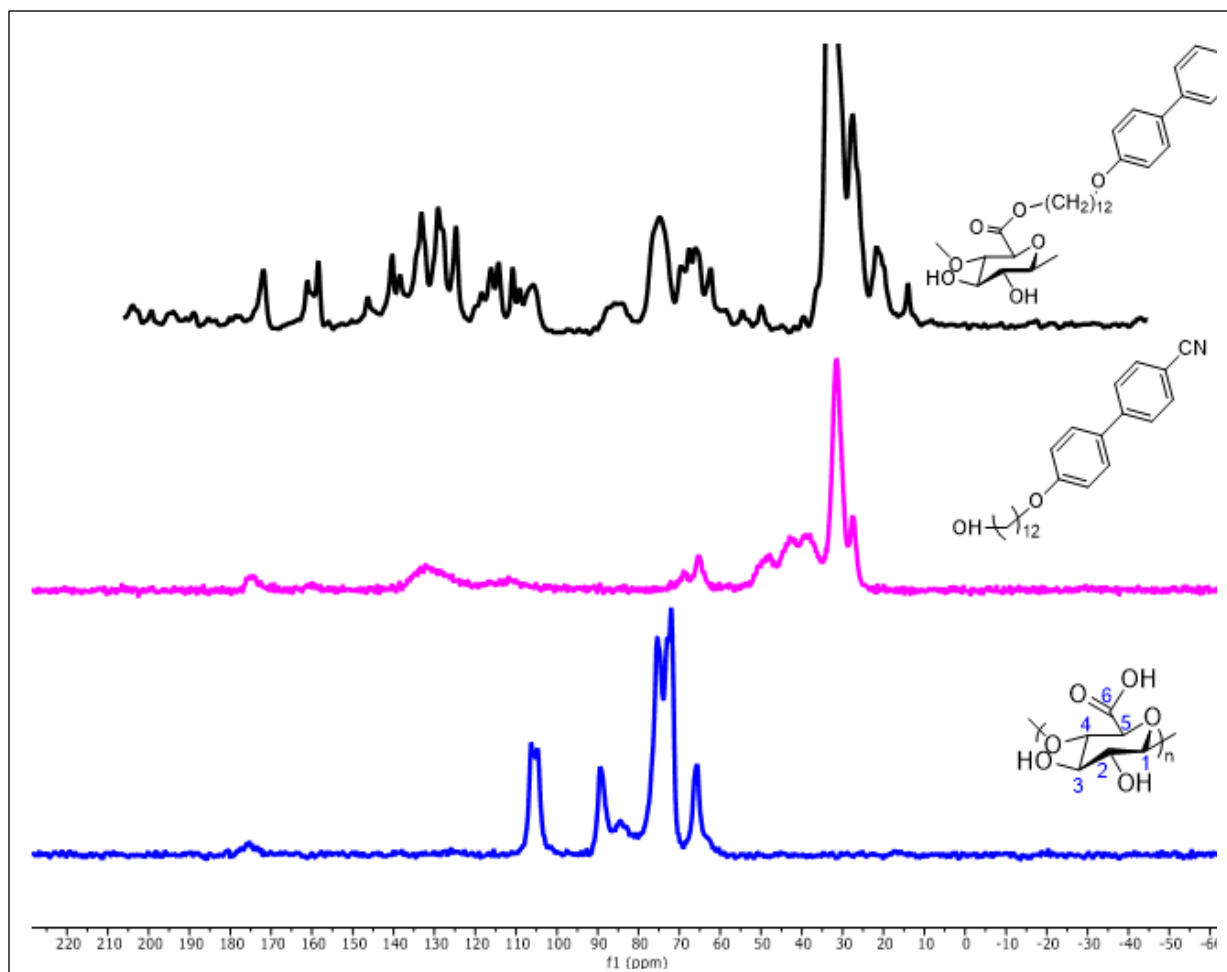


**Figure S2.** Solid-state cross-polarization  $^{13}\text{C}$  NMR spectra overlay of **CNC-COOH**, **CB12**, and **CNC-COO-CB12** at  $25^\circ\text{C}$ . The **CB12** shows the aliphatic peaks between 50 ppm and 20 ppm, the aromatic-C peaks between 140 to 130 ppm. **CNC-COOH** shows the carbonyl peak at 180 ppm. The **CNC-COO-CB12** shows the aliphatic peaks between 50 ppm and 20 ppm, the aromatic-C peaks between 140 to 130 ppm in addition to the CNC peaks between 115 ppm and 60 ppm indicating the proof of functionalization.

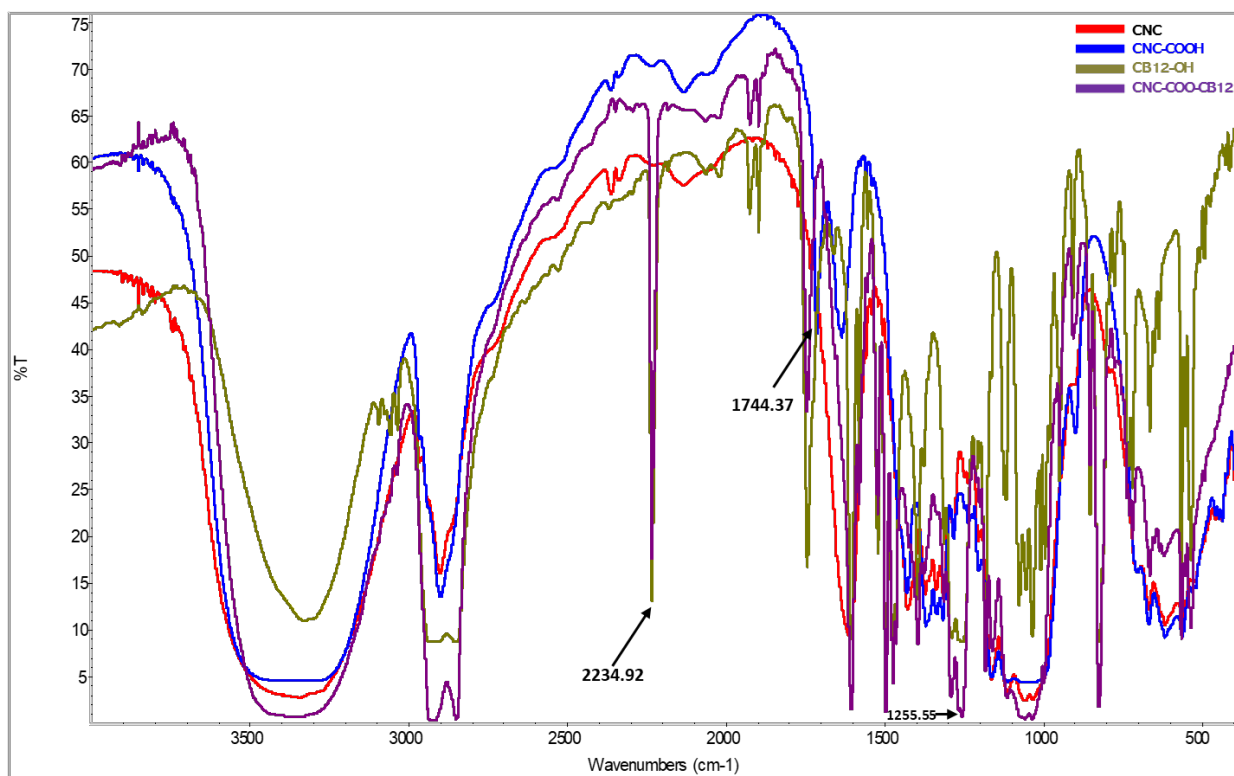


**Figure S3.** FTIR-ATR spectra overlay of CNC, CNC-COOH, CB12OH, and CNC-COO-CB12 pellets at 25°C. Oxidation of CNC is confirmed by the presence of C=O stretching at 1744.37 cm<sup>-1</sup>. The presence of CN stretching at 2234 cm<sup>-1</sup> from the CB12-OH and C-O stretching at 1255.55 cm<sup>-1</sup> confirm the formation of CNC-COO-CB12.

<b>Sample</b>	<b>Crystallinity Index (%)</b>	<b>Crystallite size (nm)</b>
CNC	86.9	6.3
CNC-COOH	80.4	7.1
CB12-OH	91.3	17.7
CNC-COO-CB12	50.3	18.7

**Table 1:** Crystallinity and crystallite size of **CNC**, **CNC-COOH**, **CB12-OH**, and **CNC-COO-CB12**



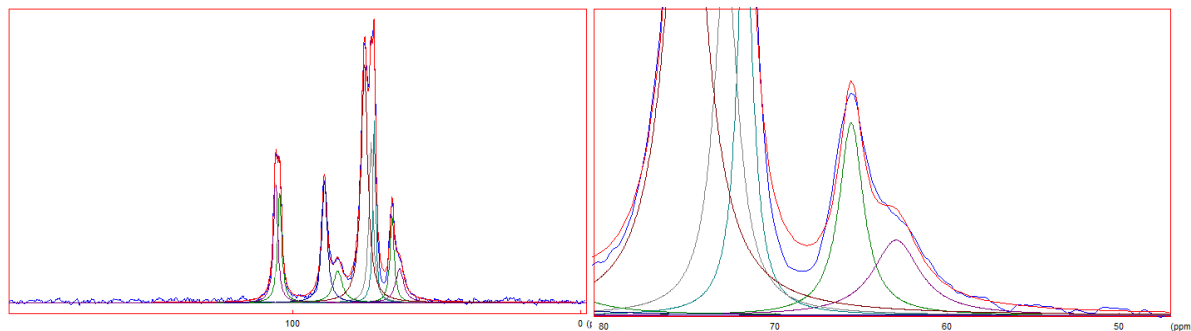


**Figure S4:** Deconvoluted  $^{13}\text{C}$  NMR spectrum of CNC obtained at 600 MHz while spinning at 35 kHz. The deconvolution was performed using the dmFit software.<sup>1</sup> The one-dimensional spectrum shows eight resolved carbon lines that can be ascribed to the different carbon sites of the structure.

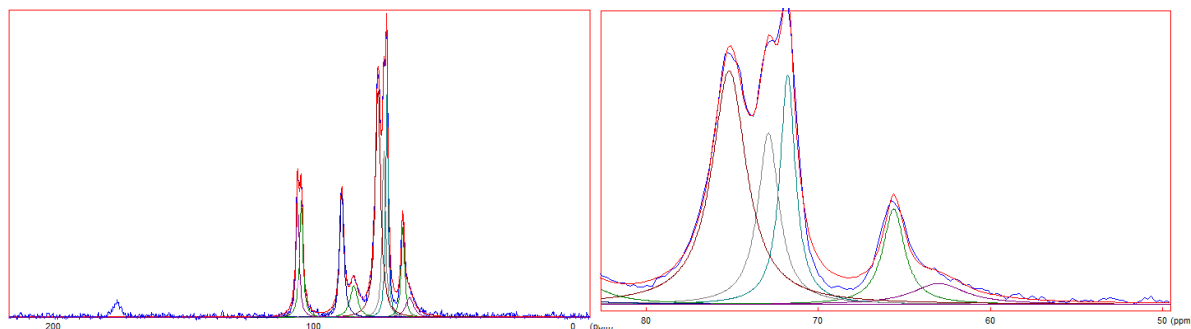


**Figure S5:** Deconvoluted  $^{13}\text{C}$  NMR spectrum of CNC-COOH obtained at 600 MHz while spinning at 35 kHz. The deconvolution was performed using dmFit software.<sup>1</sup> The one-dimensional spectrum shows eight resolved carbon lines that can be ascribed to the different carbon sites of the structure.

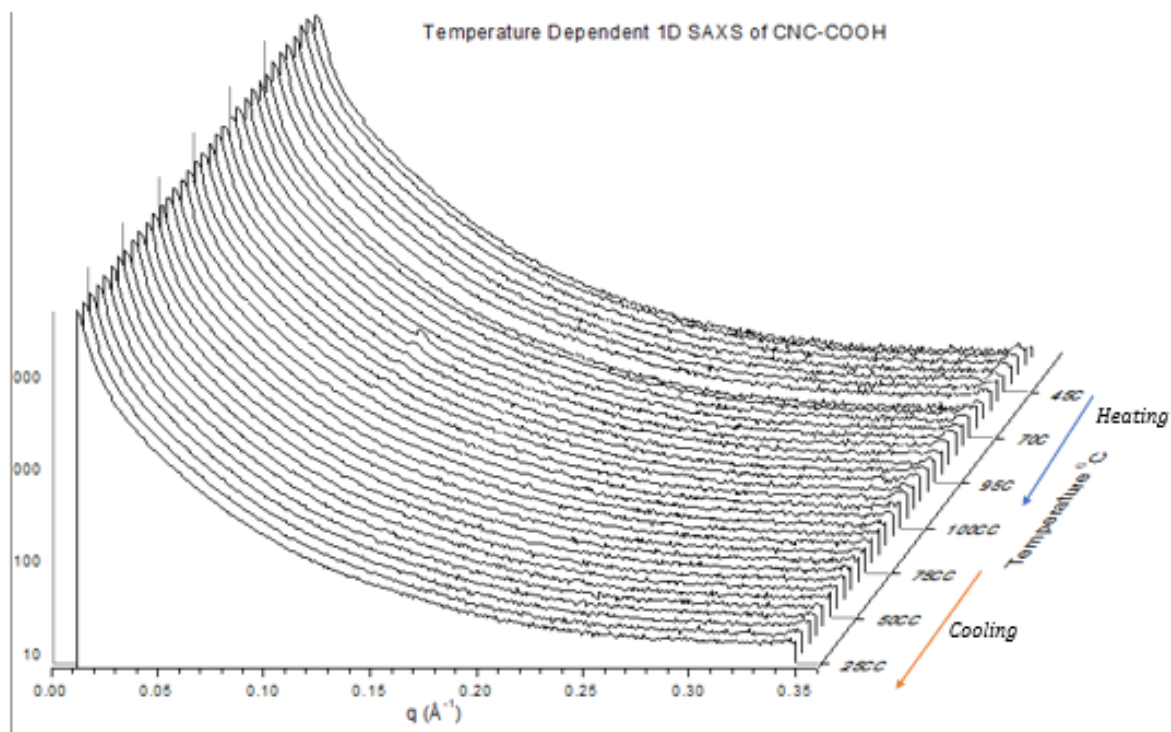


**Figure S6:** Temperature-dependent 1D SAXS of CNC-COOH powder sandwiched between the two Kapton films prepared at room temperature. The SAXS profile does not show any reflections pertinent to smectic domains.

## Morphology of the CNC and its Derivatives

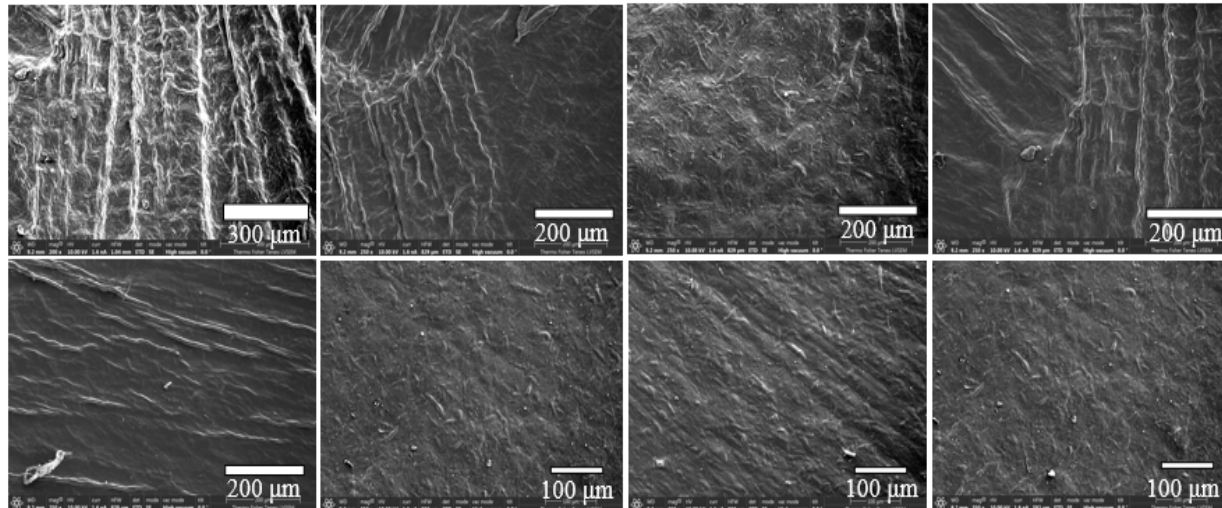
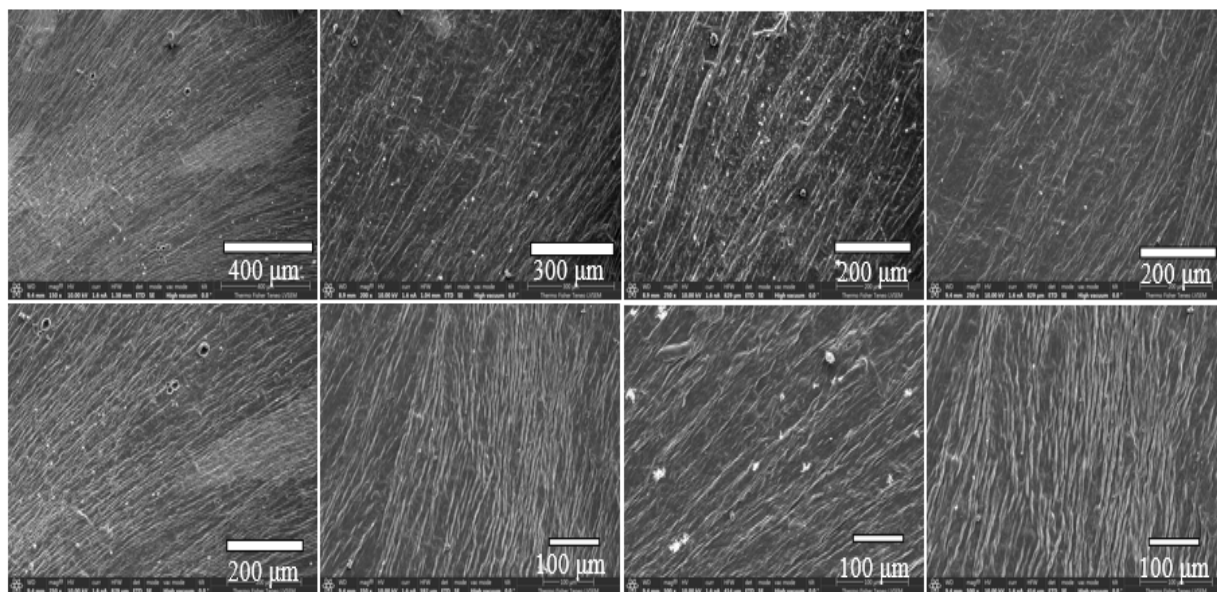


**Figure S7:** SEM images of the surface view of the 3w% CNC films prepared in LiCl/DMAc solution by drop casting technique after sonication. These images with different magnification scales display chiral nematic organization that possibly collapsed during the drying process to aggregate into rod-like structures.<sup>2</sup>



F

**Figure S8:** SEM images of the surface view of the **3w% CNC-COOH** films prepared in LiCl/DMAc solution by drop casting technique after sonication. These images with different magnification scales display chiral nematic organization that collapsed during the drying process to aggregate into rods-like structures.<sup>2</sup>

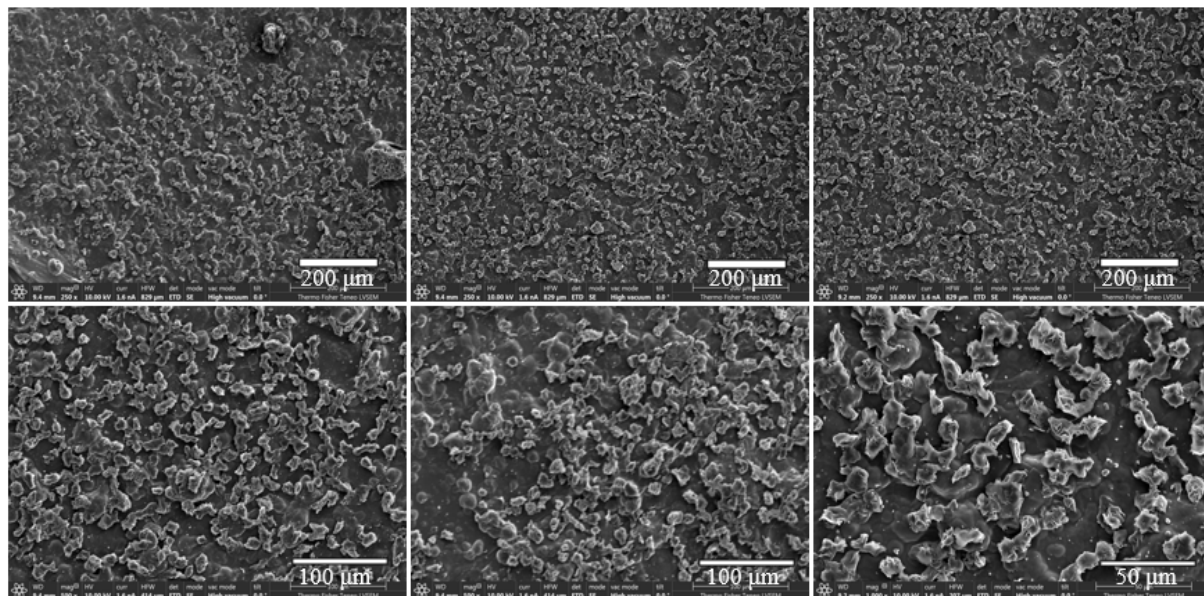


**Figure S9:** SEM images of the surface view of the 3w% CNC-COO-CB12 films prepared in LiCl/DMAc solution by drop casting technique after sonication. These images with different scale bars lack the chiral nematic organization observed in the CNC and CNC-COOH films. However, they present textured domain arrangements with topological defects.<sup>3</sup>

### References

1. Massiot, D.; Fayon, F.; Capron, M.; King, I.; Le Calvé, S.; Alonso, B.; Durand, J. O.; Bujoli, B.; Gan, Z.; Hoatson, G., Modelling one-and two-dimensional solid-state NMR spectra. *Magnetic Resonance in Chemistry* **2002**, *40* (1), 70-76.
2. Wang, P.-X.; Hamad, W. Y.; MacLachlan, M. J., Structure and transformation of tactoids in cellulose nanocrystal suspensions. *Nature Communications* **2016**, *7* (1), 1-8.
3. Honglawan, A.; Beller, D. A.; Cavallaro, M.; Kamien, R. D.; Stebe, K. J.; Yang, S., Topographically induced hierarchical assembly and geometrical transformation of focal conic domain arrays in smectic liquid crystals. *Proceedings of the National Academy of Sciences* **2013**, *110* (1), 34-39.